Article in Press

https://doi.org/10.1038/s44303-026-00196-1

Electrical impedance tomography beyond the icu: wearable architectures and AI under translational constraints

Check for updates

Michael Lawson[1,2], Henry Lui[1,2], Cheuk Man Ho[1,2], Desmond Y. H. Yap[3,4], Wai-Kay Seto[3,5], Bradley J. Edelman[1,3] ✉ & Russell W. Chan[1,6] ✉

Electrical impedance tomography (EIT) enables real-time functional imaging using non-ionizing currents and compact, low-cost hardware, but its clinical footprint remains largely confined to ICU lung monitoring. Advances in wearable architectures and artificial intelligence (AI) are driving EIT toward point-of-care applications, yet translation remains limited by technical and validation barriers. This review synthesizes progress in hardware, reconstruction, and AI-enabled analysis, and outlines a roadmap for advancing EIT toward scalable multi-organ imaging.

Primary care serves as the first point of contact for individuals and families in continuous healthcare delivery. This requires preventive screening and chronic disease monitoring outside of hospitals, and forms the foundation of the pyramid of healthcare services that leads to specialized secondary and tertiary healthcare. As populations age and the prevalence of chronic conditions increases, there is a growing demand for accessible diagnostic technologies capable of repeated, low-risk functional monitoring outside of clinical environments. However, most advanced imaging modalities remain resource-intensive and are not easily deployable in decentralized settings.

Biomedical imaging technologies such as plain radiography, computed tomography (CT), magnetic resonance imaging (MRI), and ultrasound have revolutionized structural diagnostics by providing critical insights into the anatomical structures of the human body[1–3]. These modalities all involve trade-offs related to ionizing radiation, cost, equipment size, operator dependence, or acquisition time that limit their feasibility for frequent longitudinal assessment. By contrast, functional imaging offers insights by visualizing temporally resolved physiological and metabolic activities within biological tissue. Common technologies include functional MRI (fMRI)[4], functional ultrasound (fUS)[5], positron emission tomography (PET), and single photon emission computed tomography (SPECT)[6]. These modalities are in varying stages of clinical maturity, but all still rely on specialized infrastructure, expensive instrumentation, or radiotracers.

Electrical impedance tomography (EIT) offers a fundamentally different approach. By measuring tissue impedance variations through surface electrodes, EIT enables non-ionizing, real-time functional imaging using compact and relatively low-cost hardware[7]. While historically limited to pulmonary monitoring in intensive care settings, recent advances have substantially expanded its technical capabilities. We argue that EIT is entering a point-of-care phase[8] driven by converging forces that include miniaturized hardware[9], artificial intelligence (AI)-based reconstruction and processing strategies[10,11], and the emergence of wearable architectures[12,13]. However, its scalable deployment across hospital, community, and home-based monitoring contexts will depend on overcoming five critical barriers: (i) boundary variability and electrode-tissue interface instability, (ii) forward-model mismatch in heterogeneous or deep organs, (iii) AI generalization limits arising from scarce and non-standardized multicenter datasets, (iv) the need for longitudinal reproducibility and drift control in chronic monitoring, and (v) rigorous validation of EIT-derived biomarkers against established clinical reference standards (Fig. 1). In this review, we synthesize recent progress in hardware design, reconstruction/processing methodologies, and AI-enabled analysis through the lens of these challenges and outline practical criteria for advancing EIT toward scalable functional imaging beyond specialized clinical settings.

Physical and architectural limits of EIT resolution

The drive for disease detection has historically relied on imaging techniques such as plain radiography, CT and MRI. These approaches have demonstrated that early intervention can lead to better prognosis and reduced healthcare costs; however, they are infrastructure-intensive and may not be optimized for repeated monitoring in decentralized settings. EIT offers a complementary strategy that prioritizes repeatability, safety, and temporal continuity rather than maximizing structural resolution by providing low-cost, noninvasive functional imaging. Unlike traditional imaging modalities that require significant financial investment and infrastructure, the portability, low cost, and minimal hardware requirements of EIT make it uniquely suited for repeated physiological assessment. This flexibility

[1]E-SENSE Innovation & Technology, Hong Kong, China. [2]Hong Kong Centre for Cerebro-cardiovascular Health Engineering, Hong Kong, China. [3]Department of Medicine, School of Clinical Medicine, The University of Hong Kong, Hong Kong, China. [4]Queen Mary Hospital, Division of Nephrology, Hong Kong, China. [5]State Key Laboratory of Liver Research, The University of Hong Kong, Hong Kong, China. [6]School of Biomedical Engineering, The University of Hong Kong, Hong Kong, China. ✉e-mail: brad@esense-inno.tech; russell@esense-inno.tech

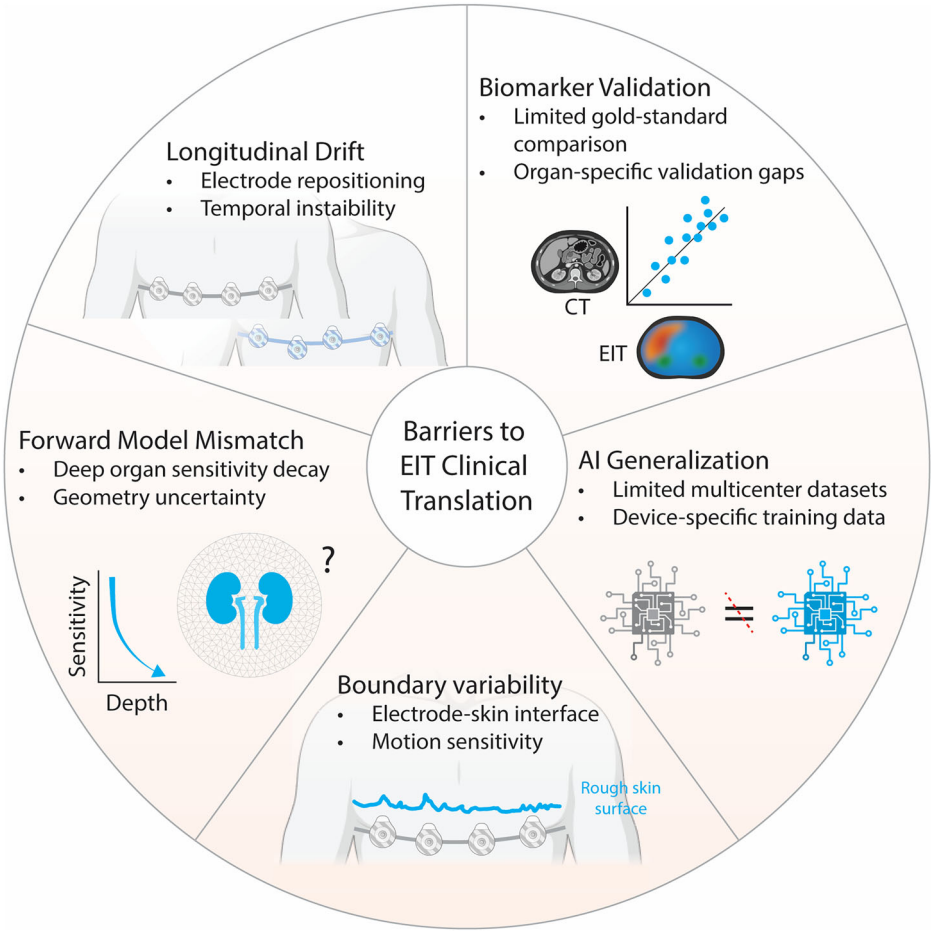


Fig. 1 | Key barriers to clinical translation of electrical impedance tomography (EIT). The principal challenges are: (1) Boundary variability arising from electrode-skin interface instability, motion sensitivity, etc., (2) Reduced sensitivity of forward-modeling for deep organs and geometric uncertainty in heterogeneous tissues, (3) AI generalization limits stemming from limited multicenter datasets and device-specific training distributions that hinder cross-device robustness, (4) Longitudinal drift from electrode repositioning and temporal instability during chronic monitoring, and (5) Biomarker validation gaps between EIT and gold-standard clinical reference measurements, as well as incomplete organ-specific validation. Together, these barriers define critical areas that require coordinated advances to enable scalable EIT deployment. Some images were created in BioRender. *Edelman, B.* (2026) https://BioRender.com/ajkeelo.

facilitates imaging of most vital organs within the thorax and abdomen (e.g., lungs, heart, liver, kidney, etc.)[14–17]. Diseases affecting these organs require continuous monitoring over the course of weeks or months, and EIT can provide a suitable option for this exact application.

The modern architecture of EIT systems is deeply rooted in developments from the 1980s, particularly the Sheffield Mark 1 prototype[18] and the adjacent pair-drive configuration introduced by ref. 19. The 16-electrode "Sheffield protocol" remains the dominant clinical architecture and defines a characteristic spatial resolution of ~15% of the belt diameter (~2–3 cm in adults)[20]. While this architecture has enabled real-time pulmonary monitoring, it also imposes an inherent resolution and depth-sensitivity ceiling that has limited applications to other organs. Subsequent innovations in electrode technology, stimulation patterns, multi-frequency acquisition, and reconstruction algorithms have improved image reliability and robustness. However, the boundary-driven nature of the inverse problem continues to constrain image fidelity in heterogeneous or deep tissues. As a result, recent innovation has increasingly shifted toward algorithmic and AI-based reconstruction strategies aimed at extending performance beyond these traditional limits.

EIT hardware architecture and deployment constraints

Hardware modules and components

EIT systems comprise several key hardware components, including electrode arrays, signal generators, data acquisition systems, amplification circuitry and computing modules. The electrode array is a crucial component of EIT systems, consisting of multiple electrodes placed around the body part being imaged. These electrodes inject small electrical currents and measure the resulting voltages. Increasing electrode count reduces angular sampling gaps and increases independent measurements, which is thought to theoretically improve spatial discrimination. However, empirical gains plateau beyond moderate electrode counts (e.g., 16–32 electrodes), with improvements manifesting primarily as peripheral noise reduction rather than central resolution enhancement[21,22]. Importantly, image quality and spatial resolution also highly depend on other reconstruction parameters, such as mesh resolution and regularization parameters[23]. In the latter case, smaller regularization parameters can improve spatial resolution due to less smoothing, but also suppress noise less.

Electrode positioning and surface characteristics can also influence the quality of the reconstructed image. Misplacement or inaccurate tracking of electrode locations can introduce geometric distortions[24–26]. In addition, poorly manufactured electrodes with size variations and small or inconsistent contact areas can limit uniform current injection, whereas wide electrode shapes may restrict the number of electrodes that can be used, and can limit spatial resolution and sensitivity to localized conductivity changes[27]. Although high-conductivity materials and optimized surface geometries mitigate these effects, boundary uncertainty remains a persistent source of reconstruction variability[23,27]. Aside from these parameters, advances in electrode design have led to the development of flexible and biocompatible materials, enhancing patient comfort and signal quality.

Modern EIT systems use highly sensitive electronics capable of capturing minute voltage changes. Current injection and voltage acquisition modules determine signal-to-noise characteristics and dynamic range. Modern EIT devices employ precision data acquisition systems and high-input impedance differential amplification to preserve boundary voltage fidelity. While advances in low-noise electronics and real-time processing have enabled bedside and portable implementations, measurement stability remains constrained by electrode interface variability rather than amplifier performance alone. Measurement amplification is often necessary to provide the appropriate voltage levels for the data acquisition system (DAQ) and to prevent loading effects. In this way, current isn't drawn from the

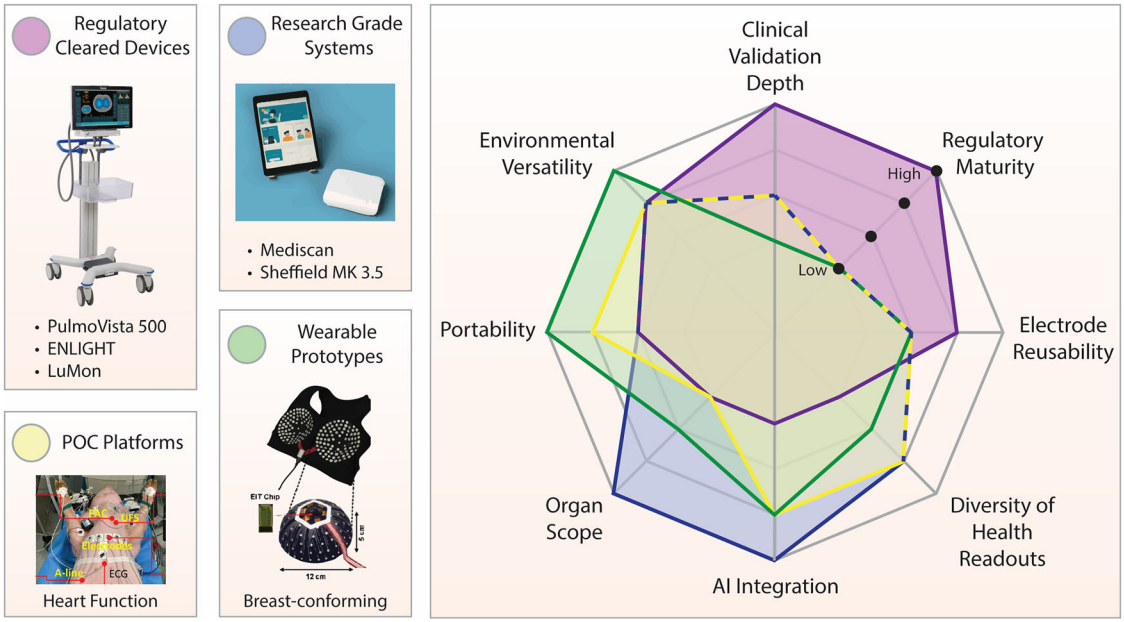


Fig. 2 | Capability trade-offs of EIT device archetypes. Comparison of regulatory-cleared devices, research-grade systems, proof-of-concept (POC) platforms, and wearable prototypes across eight functional dimensions: portability, regulatory maturity, electrode reusability, organ scope, AI integration, clinical validation depth, environmental versatility, and diversity of health readouts. Radar plots illustrate characteristic capability profiles of each archetype. Commercial systems emphasize regulatory maturity and clinical validation, whereas wearable and POC platforms prioritize portability and environmental versatility. Research-grade systems focus on expanding organ coverage, AI integration, and diversifying health readouts. Some images were reproduced from refs. 31,36–38 under the terms of the Creative Commons Attribution 4.0 International License (CC BY 4.0).

system itself and the true voltage distribution, including boundary voltages, is preserved throughout the imaging volume[28]. With these measurements, real-time reconstruction is facilitated by increasing computational efficiency; however, algorithmic stability remains the dominant determinant of image quality.

Hardware-algorithm dependence

While incremental improvements in electrode count, amplification circuitry, and DAQ sensitivity have enhanced signal fidelity, hardware upgrades alone cannot overcome the intrinsic ill-conditioning of the EIT inverse problem. Increasing electrode density, for example, may improve sensitivity at the periphery of the image and the delineation of objects therein, but does not fundamentally alter the exponential decay of sensitivity toward the image center. Similarly, reductions in contact impedance and electrical noise improve data quality, yet reconstruction accuracy remains strongly dependent on regularization strategy and forward-model assumptions. These considerations highlight the need to design EIT hardware and algorithms together, in which acquisition architecture, stimulation patterns, and reconstruction frameworks are optimized jointly rather than sequentially.

Existing EIT devices

The ideal point-of-care EIT device would meet World Health Organization (WHO) REASSURED guidelines[29], however, several devices currently used in clinical and research settings do not conform completely to these standards. These devices are designed with varying configurations of features such as portability, electrode configuration, and clinical integration. Currently available EIT systems fall into several distinct architectural archetypes that reflect different priorities. Broadly, these can be categorized as: (1) Regulatory-cleared clinical systems optimized for safety and ventilation guidance; (2) Research-grade platforms optimized for algorithm development and flexibility; (3) Wearable prototypes optimized for portability; and (4) Proof-of-concept-targeted platforms optimized for disease-specific biomarker extraction. Regulatory-cleared systems such as ENLIGHT (Timpel)[30,31], PulmoVista 500 (Dräger)[32], and LuMon (Sentec)[33] exemplify the clinical archetype by emphasizing usability for bedside lung monitoring in ICUs (e.g., ventilation titration and perfusion assessment). On the other hand, research-grade systems like the Sheffield MK 3.5 (Maltron)[34] and Mediscan (Gense Technologies)[35,36] represents a lower-cost, development-stage option, that often target broader organ monitoring (lung, liver, kidney) with machine learning-enhanced analysis. Finally, wearable prototypes and proof-of-concept systems target specific biomarkers, for example, of the heart[37], with clinical reference verification, or aim to optimize ergonomic factors by conforming to bodily curvature[38]. These archetypes reveal a fundamental trade-off landscape between stability and ease-of-use in the clinic, and innovation involving AI analytics and novel organ targets (Fig. 2).

What current devices reveal about field limitations

Despite technological maturation, commercially available EIT systems exhibit several recurring architectural characteristics that reflect unresolved issues across the field. First, most devices deployed in the clinic rely on 16–32 electrode configurations using adjacent or near-adjacent drive patterns, reinforcing a practical but resolution-limited paradigm. While adequate for thoracic imaging of the lungs, this architecture constrains spatial fidelity and depth sensitivity in heterogeneous or deeper abdominal organs. Second, regulatory-approved systems remain predominantly optimized for pulmonary applications, with relatively limited validation in cardiac, renal, or hepatic contexts. Third, standardized multicenter datasets for benchmarking reconstruction performance across devices and patient populations are largely absent. Finally, although AI-enhanced analysis is increasingly reported in research settings, integration of data-driven reconstruction methods into clinical devices remains limited. Collectively, these patterns indicate that incremental hardware evolution has not yet altered the fundamental resolution-stability ceiling imposed by boundary-driven reconstruction.

Regulatory pathway

The regulatory pathway for EIT devices involves rigorous testing and compliance with medical device standards to ensure safety, efficacy, and reliability. Different regions have specific regulatory requirements that

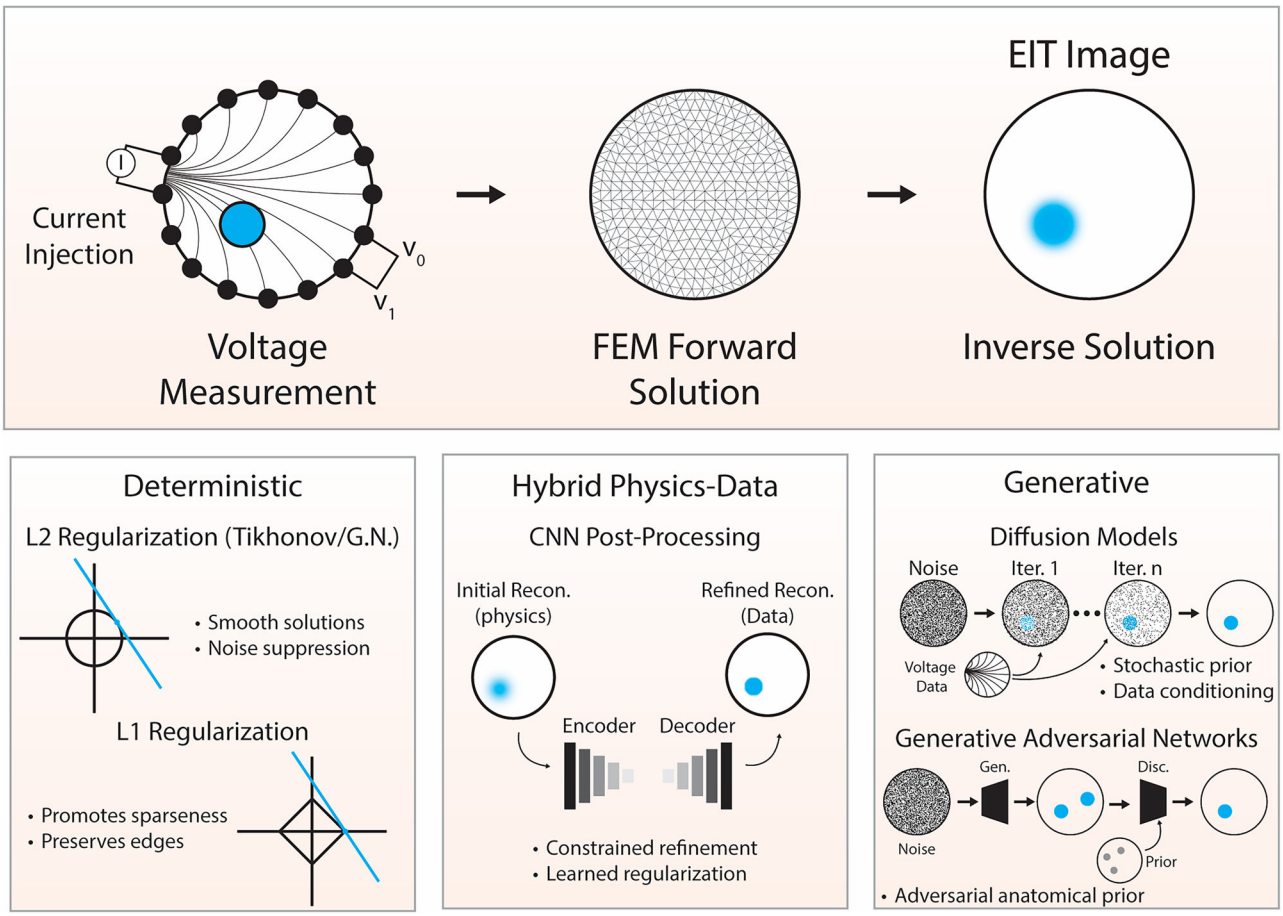


Fig. 3 | EIT reconstruction and inverse solver taxonomy. (top row) Standard EIT processing pipeline from current injection and boundary voltage measurement to forward modeling via finite element methods (FEM) and inverse reconstruction of conductivity images. (bottom row) Conceptual categorization of inverse solvers. (left) Deterministic methods (L2- and L1-norm) impose explicit mathematical priors such as smoothness or sparsity. (middle) Hybrid approaches apply learned refinement (e.g., CNN postprocessing) while retaining physics-based constraints. (right) Generative methods, including diffusion models and generative adversarial networks (GANs), introduce learned anatomical priors that aim to reshape solutions beyond direct measurement constraints.

manufacturers must meet to market their devices; the United States employs the Food and Drug Administration (FDA), Europe requires compliance with the medical device regulation (MDR) and CE marking, and China regulates devices by the National Medical Products Administration (NMPA). As EIT systems increasingly incorporate AI-driven reconstruction and biomarker inference, regulatory expectations are likely to expand beyond hardware safety and basic performance standards. Prospective multicenter validation studies and reproducibility across repeated measurements will also likely be required to establish clinical equivalence with established reference standards. These considerations highlight the growing convergence between device and algorithm development, and regulatory standards in the next phase of EIT development.

Ongoing hardware developments

Overcoming the resolution-stability trade-off in EIT will likely require innovations that couple material science advances with acquisition and reconstruction strategies. One of the most promising directions is the development of more advanced electrode materials and designs. Current research is exploring the use of graphene and carbon nanotubes for electrode arrays due to their superior conductivity, flexibility, and biocompatibility[39]. Compared to traditional silver/silver-chloride electrodes, these materials exhibit a higher surface area and conductivity, which can reduce contact impedance, thermal noise, and resistive loss, and can therefore facilitate smaller electrode size (and higher density arrays) while maintaining low impedance[40,41]. All of these qualities can improve the quality of the electrical signal captured by an EIT system, and may improve boundary signal stability and enable more dense electrode layouts.

EIT data processing and analysis

Fundamental constraints of the EIT inverse problem

The process of EIT image reconstruction involves converting surface voltage measurements into cross-sectional images of internal conductivity distributions (Fig. 3). EIT reconstruction is fundamentally limited by the mathematical properties of the underlying inverse problem. Unlike tomographic modalities that rely on line integrals (e.g., CT), EIT measurements reflect diffuse current propagation governed by partial differential equations. As a result, multiple internal conductivity distributions can produce nearly indistinguishable boundary voltage measurements, rendering the inverse problem non-unique, ill-conditioned, and sensitive to measurement perturbations.

Several intrinsic constraints define EIT performance. First, non-uniqueness and instability imply that small perturbations in measured voltages can lead to disproportionately large variations in reconstructed conductivity. Regularization techniques stabilize solutions but also introduce smoothing and bias, enforcing a trade-off between spatial resolution and noise suppression. EIT also exhibits exponential decay of sensitivity with depth, meaning that current density is highest near the boundary electrodes and diminishes toward the center of the imaging field. Consequently, superficial conductivity changes are detected more reliably than deep perturbations, which limits accuracy when imaging large or heterogeneous organs.

In addition to reduced depth sensitivity, conventional EIT does not reconstruct a true two-dimensional image plane. Rather, each reconstructed slice represents a weighted volume that extends slightly above and below the electrode plane, and which results in a lens-shaped imaging region[42]. Consequently, conductivity changes outside the nominal imaging plane may in fact contribute to the reconstructed image, introducing partial-volume effects and reducing anatomical specificity[43]. This effect becomes increasingly important when imaging large or heterogeneous organs, where out-of-plane structures may influence measured boundary voltages.

From the modeling side, boundary shape uncertainty can introduce systematic reconstruction error. Accurate forward modeling requires precise knowledge of electrode positions and body geometry. Even minor discrepancies between assumed and true boundary conditions can propagate into image artifacts or spatial distortion[44]. Compounding this, biological tissues are neither homogeneous nor isotropic, and often violate the simplified assumptions commonly used in forward models. These mismatches introduce systematic model error that cannot be fully compensated by increased mesh density or computational refinement.

These constraints collectively define a resolution-stability trade-off that has historically limited EIT to qualitative or relative imaging tasks. Overcoming this ceiling will require coordinated advances in acquisition architecture, forward modeling, and data-driven reconstruction strategies rather than incremental improvements in any single component.

EIT image reconstruction

Building upon these intrinsic constraints, reconstruction algorithms aim to approximate stable conductivity estimates largely by balancing model fidelity and computational complexity with regularization biases (Fig. 3). Various algorithms have been developed to tackle EIT reconstruction, which involves solving both the forward and inverse problems. The finite element method (FEM)[45] is widely used for solving the forward problem by modeling complex geometries and heterogeneous conductivity distributions within a volume, and subsequently generating a tessellated solution space of varying resolutions. By contrast, the boundary element method (BEM) is a similar approach, but models a volume as piecewise shells of homogeneous conductivity values[46]. The simplicity of BEM can significantly speed up solving the forward solution; however, the lack of modeling detail can produce crude reconstructions compared to the fine volume-wide meshes created by the FEM.

Classical inverse approaches range from linear back-projection (LBP) to iterative Newton-type solvers. LBP[47] was one of the earliest EIT reconstruction methods and benefited from being simple and fast, but suffers from low spatial resolution and high susceptibility to noise. Regularization methods using L1-, L2- (Tikhonov), or mixed-norm regularization, are also employed to stabilize the inverse problem by incorporating prior information or constraints into the reconstruction process[48–50]. L2-based Tikhonov regularization stabilizes inversion but enforces global smoothness that may obscure sharp conductivity transitions, whereas L1-based methods better preserve boundaries, but at the expense of parameter sensitivity and computational cost. Alternatively, algorithms such as Gauss–Newton[51] and conjugate gradient[52] iteratively refine the conductivity distribution to minimize the difference between measured and computed voltages. While more computationally intensive and sensitive to noise, these methods generally produce higher quality images and more accurate reconstructions compared to non-iterative counterparts .

Physiological parameter extraction

Signal processing enhances boundary voltage stability through filtering, artifact correction, and drift compensation prior to reconstruction[53–55]. Quantitative analyses measuring parameters such as regional conductivity changes can indicate physiological or pathological conditions in pulmonary and perfusion disorders[56,57]. Functional imaging that assesses dynamic changes in conductivity over time is also useful for monitoring processes like respiration[58] or perfusion[59]. Furthermore, comparative analysis validating EIT against other imaging modalities (e.g., MRI and CT) can improve diagnostic accuracy by enhancing the reliability and confidence in EIT data interpretation. Specifically, comparative analyses between EIT and imaging techniques with higher resolution may help distinguish modality-specific artifacts from true physiological phenomena to mitigate misdiagnoses and establish a data-driven range for diagnostic sensitivity and specificity.

Commercial EIT systems, such as those used for lung monitoring, typically focus on specific measurements and parameters that clinicians have found most useful in practice[60]. Clinically adopted metrics such as the *Global Inhomogeneity Index*[61] and *Silent Spaces*[62] quantify spatial heterogeneity of ventilation and guide ventilator titration in acute respiratory distress syndrome (ARDS) and management of chronic obstructive pulmonary disease (COPD). Moreover, *End-Expiratory Lung Impedance*[63] and *Regional Ventilation Distribution*[64] indicate changes in lung volume and ventilation distribution, respectively, and help optimize mechanical ventilation strategies.

In addition to these well-established metrics, preclinical EIT research has identified additional useful parameters based on either time-difference EIT (tdEIT) or frequency-difference EIT (fdEIT)/spectroscopic EIT. Time-difference EIT can effectively detect changes in conductivity over time and/or between physiological states, such as during a respiratory or heart cycle. Frequency-difference or spectroscopic EIT utilizes multiple frequencies to identify tissue type and content based on frequency-specific signatures. Importantly, tdEIT and fdEIT approaches partially mitigate depth sensitivity limitations by exploiting temporal or frequency-dependent contrast rather than absolute conductivity values. They can also be combined with statistical techniques such as principal component analysis or eigen decomposition to extract features specific to individual organs (e.g., separating cardiac and pulmonary signals from thoracic recordings)[65,66].

Open-source processing tools

Open-source processing tools such as EIDORS[67] and PyEIT[68] have standardized forward modeling and reconstruction approaches through simulation workflows. The availability of open-source frameworks has accelerated algorithm innovation and benchmarking, yet the absence of universally adopted datasets limits objective performance comparisons across multiple studies. Nevertheless, these tools have democratized EIT research, enabling more researchers to contribute to the field.

The integration of artificial intelligence with EIT

AI in EIT image reconstruction

The application of deep learning techniques to EIT imaging aims to address low spatial resolution and sensitivity to noise that is inherent to traditional reconstruction methods (Fig. 3). CNN-based postprocessing has demonstrated improved visual fidelity; however, most implementations function as refinement layers without fundamentally changing the ill-conditioning imposed by the forward model[69–72]. For example, Deep D-bar uses a CNN to sharpen blurred D-bar outputs to improve the identification of anatomical boundaries without modifying the original inverse solver[69]. Finally, CNNs have also been used in combination with classical reconstruction methods by enabling the network to self-tune regularization weights and hyperparameters to improve noise robustness and generalization[73]. Related architectures, such as autoencoders, have been shown to suppress boundary noise while preserving conductivity contrasts[74], and stacked autoencoders can lead to higher diagnostic accuracy of breast tumors compared to traditional classifiers[75].

Building upon these learned feature representations, GAN-based approaches incorporate anatomical priors, most often of the lungs, directly into reconstruction[76,77]. Unlike many CNN-only approaches, GAN-based methods often fold the prior into the inverse reconstruction process, which can improve perceptual realism but risks over-constraining solutions toward anatomically typical patterns. Conditional GANs have also been shown to improve the reconstruction of thoracic phantom maps compared to traditional Tikhonov- and CNN-based reconstructions under high noise conditions[78]. Image-to-image translation frameworks such as CycleGAN have also been used to generate MRI- or CT-like representations from EIT

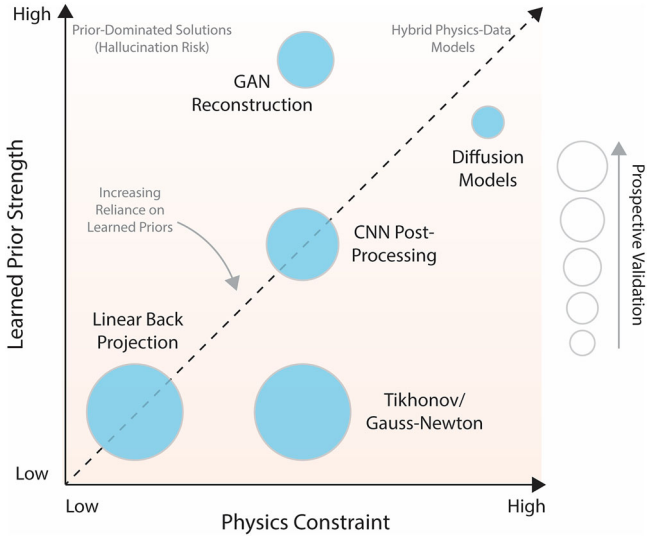


Fig. 4 | Spectrum of EIT reconstruction approaches. Conceptual map of inverse solver classes across the degree of physics constraint enforced during reconstruction (x-axis) and the strength of learned data priors influencing the solution (y-axis). Deterministic solvers such as linear back-projection and Tikhonov/Gauss–Newton methods emphasize measurement consistency. Generative methods, exemplified here by GANs and diffusion models, also include related latent variable approaches such as variational autoencoders. The dashed diagonal indicates the increasing overall reliance on learned priors.

inputs[79,80]. While these approaches enhance anatomical plausibility, for example by improving fat and bone conductivity estimates in the wrist or by providing a more detailed assessment of the lungs, they blur the distinction between measurement-derived reconstruction and modality synthesis.

At the high end of the generative spectrum, diffusion-based methods have shown that reconstructed EIT conductivity maps conditioned on voltage data outperform both CNN and GAN methods on synthetic and real datasets[81,82]. Building on this, recent diffusion-based methods such as DiffusionEIT and diffusion-regularized implicit representations (Diff-INR) demonstrate stronger robustness to noise, better generalization, and improved spatial fidelity[81,83]. Moreover, hybrid diffusion strategies like SDEIT (which uses a Stable Diffusion prior) and DUMD-EIT (which applies masked diffusion as a refinement step) are pushing the frontier by incorporating semantic or structural priors to steer reconstructions in a more informed way[84,85]. These developments suggest a transition toward hybrid architectures that couple stochastic generative priors with measurement-consistent constraints.

In summary, AI-based reconstruction strategies can be conceptualized along a space defined by both the degree to which reconstruction is constrained by the physical forward model and the extent to which learned priors dominate the solution (Fig. 4). Traditional deterministic solvers anchor the physics-constrained end of this spectrum, whereas generative models such as general adversarial networks (GANs) and diffusion frameworks increasingly incorporate learned anatomical priors that may reshape conductivity maps beyond direct measurement constraints. Most contemporary approaches occupy intermediate territory, coupling data-driven refinement with traditional inverse operators.

Limitations of generative and deep models in EIT

Despite impressive improvements in reconstruction fidelity, AI-driven EIT methods introduce new sources of uncertainty that warrant careful scrutiny. Deep generative models, including GANs and diffusion-based approaches, inherently learn priors from training data and may hallucinate anatomically plausible but physiologically inaccurate structures when confronted with ambiguous or noisy measurements. Because of the ill-posed nature of EIT, learned priors can dominate the solution and potentially obscure conductivity variations that do not conform to the model's learned distribution.

Domain shift presents another major challenge. EIT datasets are often acquired using specific electrode configurations, stimulation patterns, and body anatomies. Models trained on one device or population may generalize poorly to others, particularly in abdominal or heterogeneous organs, where there can be substantial anatomical variability. The scarcity of large, multicenter in vivo datasets further exacerbates this issue and limits objective benchmarking across research groups. Importantly, in addition to acquiring large EIT datasets, supervised AI models require reliable ground-truth labels[86], which for many EIT applications cannot be derived from impedance measurements alone. Instead, clinically meaningful training targets often require paired acquisition with complementary imaging modalities (e.g., CT, MRI, and ultrasound), physiological measurements (e.g., spirometry), laboratory biomarkers, or expert clinical interpretation. Generating these multimodal datasets is resource-intensive because each EIT examination must be synchronized with an appropriate reference standard and carefully annotated to accurately capture clinically relevant physiology. Even when expert annotations are successfully gathered, diagnostic ambiguity and inter-rater inconsistencies mean that verifying a definitive, gold-standard ground truth remains challenging[87].

Generative AI models can create synthetic EIT datasets that augment existing data and improve the training of DL models[77], however, over-reliance on simulated or augmented datasets may bias models toward simplified anatomical assumptions. With this being said, deep image prior approaches such as DeepEIT[88] or Deep Dynamic Image Prior (D2IP)[89] offer a way around needing large training sets by fitting a neural network directly to measurements and using the network's architecture as built-in regularization. Future progress will likely require physics-informed or constraint-aware architectures that explicitly enforce data consistency while learning structured priors.

AI-enhanced signal processing and analysis in EIT

Beyond image reconstruction, AI techniques are transforming the signal processing and analysis stages of the EIT pipeline. Traditional statistical decomposition methods have been used to extract features or reduce noise in EIT measurements, but modern AI approaches often outperform them by learning directly from the raw data. For instance, neural networks can learn discriminative features directly from raw boundary voltages, which can eliminate the need for manual feature engineering. For instance, a CNN + SVM hybrid model applied to raw EIT boundary voltages was able to distinguish apnea vs non-apnea in neonates[90]. Other works focusing on pulmonary function have utilized deep feature engineering by combining pretrained CNN backbones (e.g., ResNet-50 and DenseNet-201) with fine-tuned 3D convolutional and dense networks to classify lung disease states or ventilation modes from EIT data[91,92].

Deep learning models can also be applied to EIT time-series data to filter out noise and adapt to non-stationary artifacts more effectively than classical filters, which is particularly relevant for wearable and continuous monitoring contexts. For instance, a residual-learning network was recently used to remove periodic vibration interference in EIT data, showing superior artifact suppression compared to standard filtering techniques[93]. Recurrent neural networks (RNNs) have also shown value for EIT analysis, specifically by capturing the temporal dependencies in time-varying data often captured during physiological phenomena such as breathing cycles, pulsatile changes, etc. Architectures based on combinations of RNNs and CNNs or long short-term memory (LSTM) have shown to account for time continuity between consecutive or even more distant EIT frames to achieve smoother dynamic images and reduce frame-to-frame noise[94,95]. Other RNN-based architectures can learn mappings from impedance time series directly to physiologic parameters (e.g., flow, volume) without manual feature extraction[96]. In summary, AI-driven analysis techniques facilitate the extraction of cleaner and more meaningful information from EIT measurements, and adapt in real-time to improve the accuracy of continuous

Table 1 | Functional capabilities of AI algorithms across the EIT pipeline

EIT feature/capability	CNN/feedforward	Generative/conditional	Sequential/recurrent
Improved spatial resolution	✓[69–72].	✓[76,77,84]	-----
Improved noise robustness	✓[73,74,93]	✓[78,83,85]	✓[94]
Artifact reduction	✓[69,71].	✓[77,81,82]	✓[94,95]
Temporal modeling (dynamic)	-----	-----	✓[94–96]
Automatic feature extraction	✓[75,90–92]	✓[79]	-----
Improved anatomical realism	✓[71,74]	✓[77,80,81,84,85]	-----
Self-tuning/adaptive regularization	✓[71,73]	-----	-----
Cross-modality translation	-----	✓[79,80]	-----
Synthetic/augmented data generation	-----	✓[77,78,81]	-----
Personalized/patient-specificmodeling	-----	-----	✓[94,97,98]
Computational efficiency	✓[69].	✓[88,89]	✓[94]

organ monitoring (like tracking lung ventilation or cardiac output), where signals can be noisy and time-correlated.

Lastly, AI-driven EIT may facilitate patient-specific parameterization of reconstruction and monitoring models. Because machine learning models can incorporate patient-specific data (such as anatomy, baseline impedance, or disease characteristics), EIT systems can be tailored to an individual's profile for more accurate interpretation. In critical care, for instance, integrating AI with EIT has been suggested to optimize ventilation strategies on a per-patient basis, adjusting for each patient's lung mechanics and heterogeneity in real time[97]. Deep learning techniques can also be used to create patient-specific computational models or "digital twins" that account for anatomical variations, which can improve the accuracy of EIT reconstructions and may help titrate therapies, diagnostic plans, and health interpretations[98]. Collectively, AI-based EIT approaches encompass feed-forward convolutional architectures, generative frameworks, and sequential models, each contributing distinct capabilities. Table 1 summarizes these distinctions and highlights the complementary strengths of different AI techniques across the EIT pipeline.

Regulatory acceptance of AI-based EIT

While AI expands the scope of EIT systems, it also introduces new regulatory considerations. As algorithms move from postprocessing tools to components that aid in decision making, regulatory agencies have taken an open but cautious approach to approving AI for medical device use. EIT systems that incorporate generative or continuously learning models will face increasing scrutiny regarding transparency and realism in particular, and demonstrating algorithm stability and safety will be essential for approval of AI-assisted EIT as a diagnostic or monitoring tool.

Clinical uses of EIT

Maturity spectrum of EIT applications

EIT applications span a spectrum from established intensive care use to exploratory research domains. Framing these applications by maturity clarifies both the current clinical impact of EIT and the translational barriers that remain. Broadly, EIT applications can be grouped into: (Tier 1) established uses in critical care ventilation; (Tier 2) expanding clinical domains with growing prospective evidence; and (Tier 3) exploratory applications that remain in feasibility or early translational stages (Fig. 5).

Tier 1: Ventilation guidance in the ICU

Respiratory monitoring is the most widely used clinical application of EIT, especially for monitoring ventilation distribution and guiding mechanical ventilation in ICU patients with ARDS or other forms of respiratory failure[99]. To prevent ventilator-induced lung injury due to ventilation inhomogeneity, tidal volumes can be redistributed by individually titrating the positive end-expiratory pressure (PEEP), guided through real-time EIT monitoring[100,101]. Randomized and pilot studies suggest that individualizing PEEP with EIT can reduce harmful mechanical power and driving pressures delivered to the lungs and are associated with trends toward improved clinical outcomes, though a definitive mortality benefit remains under investigation[102,103]. While large multicenter trials are still needed, these promising results position EIT as a valuable adjunct for protective ventilation protocols in ICU practice. Not surprisingly, international surveys report that an increasing number of ICUs worldwide are implementing EIT for advanced respiratory monitoring, reflecting growing clinical acceptance[99].

Tier 2: Expanding clinical domains

Beyond adult ICU ventilation, EIT is increasingly applied in neonatal, pediatric, and perioperative respiratory management, where real-time regional ventilation assessment offers advantages over global metrics alone. Monitoring regional ventilation, changes in end-expiratory lung volume, and other metrics have been demonstrated in preterm infants and have been linked to subsequent oxygen dependence[104–107]. Feasibility studies have also shown that EIT can safely support PEEP titration and ventilation guidance similar to what is more commonly performed in adults[108,109]. Challenges such as electrode placement on small thoracic surfaces and signal stability remain barriers to widespread neonatal adoption, though feasibility and prognostic value have been demonstrated.

Intraoperative studies have demonstrated the feasibility of EIT for continuous bedside assessment of lung ventilation in patients undergoing major abdominal and laparoscopic procedures[110,111]. EIT-guided strategies for PEEP titration and protective ventilation during surgical procedures have also improved oxygenation and reduced postoperative pulmonary complications[112,113]. Beyond perioperative ventilation management, EIT has been used to detect acute events such as pulmonary aspiration under anesthesia[114], suggesting that real-time EIT feedback could play an important role in individualized perioperative respiratory management.

Tier 3: Exploratory and translational domains

Applications beyond thoracic imaging highlight both the versatility of EIT and the limitations imposed primarily by aspects such as depth sensitivity and anatomical heterogeneity. These domains remain largely investigational and serve as test cases for overcoming the fundamental constraints discussed earlier.

Renal and hepatic monitoring

Chronic kidney disease (CKD) and fatty liver disease (FLD) constitute important healthcare burdens. The high throughput of EIT holds promise for the noninvasive population screening of such chronic illnesses to enable the early identification and timely intervention for at-risk individuals. In patients with established CKD and FLD, EIT can easily be deployed for repeated measurements to monitor the progress of the disease, in both the hospital and ambulatory settings. In fact, researchers recently confirmed that EIT can detect physiologically relevant changes in ex vivo kidney

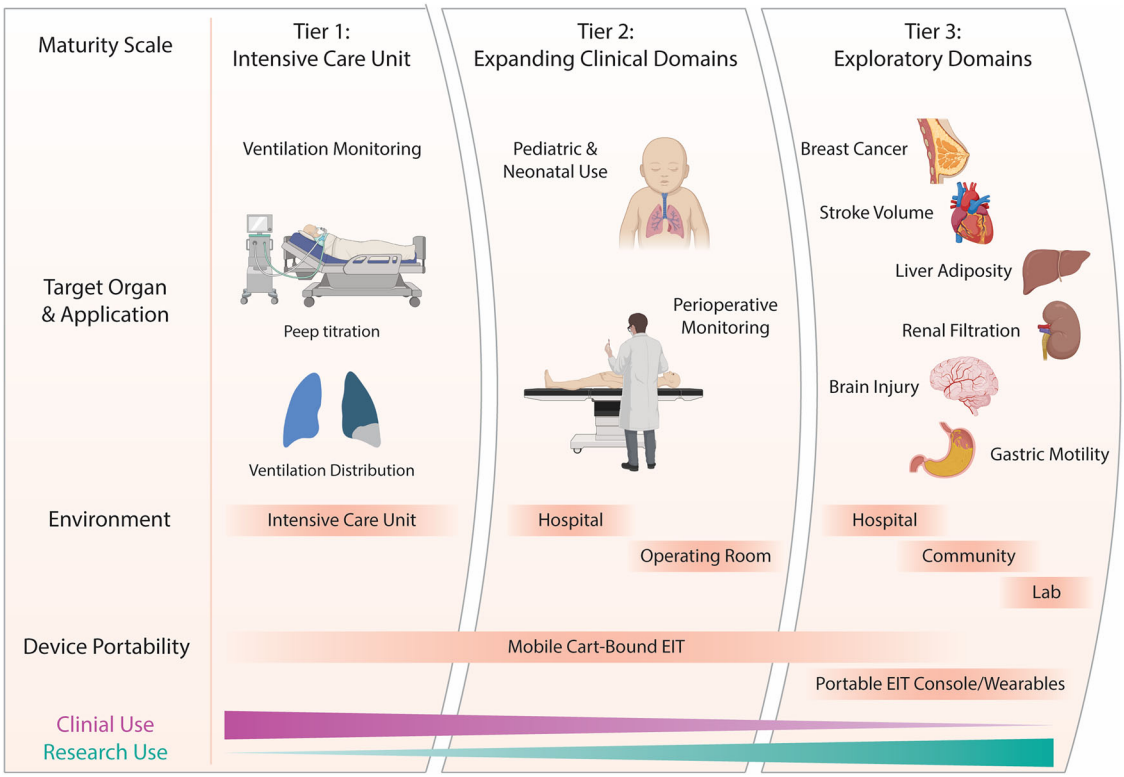


Fig. 5 | Maturity spectrum of EIT applications. Evolution of EIT from established intensive care unit (ICU) ventilation monitoring (Tier 1) toward expanding hospital-based applications (Tier 2) and exploratory organ domains (Tier 3). Applications progress from ventilation monitoring and lung-focused PEEP titration in the ICU to pediatric, perioperative, and multi-organ exploratory uses, including cardiac, hepatic, renal, neurologic, and gastrointestinal monitoring. Dark horizontal bands indicate the primary environment and desired device portability for each application tier, increasing from cart-bound systems toward wearable platforms. The lower bars indicate the transition from predominantly clinical use to research-driven expansion. Some images were created in BioRender. *Edelman, B.* (2026) https://BioRender.com/oowpkv9.

tissue[115]. In vivo results in healthy individuals and CKD patient populations suggest that EIT may be capable of detecting disease stage based on frequency-specific impedance signatures[116]. Similarly, ex vivo and in vivo hepatic EIT research in animal models being fed high- and low-diets demonstrates that fatty infiltration in the liver changes its electrical properties[117]. These changes manifest as frequency-specific EIT signatures that are also highly correlated with fat content measured by clinical MRI and elastography[16,118], and which can be used to identify different stages of MASLD. Despite these promising studies, large-scale prospective validation against gold-standard clinical metrics such as estimated glomerular filtration rate and MRI-based fat quantification remains limited, and reproducibility across anatomies and electrode configurations has not yet been systematically assessed.

Brain imaging

One of the most intriguing research frontiers is EIT-based brain imaging, which aims to monitor cerebral function and pathology non-invasively. The brain presents a challenging target for EIT due to the skull's insulating properties and the fine spatial resolution needed to detect cortical or subcortical activity. Multi-frequency EIT methods targeting the brain have shown that human neural tissue affected by various dysfunctions (e.g., ischemia and hemorrhage) can induce measurable impedance changes[119]. In rodents, EIT has been further utilized to detect regional impedance differences following experimentally induced ischemic or hemorrhagic stroke[120,121] and has mapped slow and fast epileptiform discharges with spatial specificity[122,123]. These animal experiments benefit from thinner skulls and reduced attenuation, but they also establish essential benchmarks in that transcranial signal separation is possible and that neural events leave distinct conductivity signatures. If technical challenges can be overcome in humans, EIT might ultimately permit bedside detection of evolving edema, hemorrhage, or seizures by continuously observing impedance signatures in real time.

Cancer and oncology applications

In oncology, EIT has long been investigated for its potential in tumor detection and characterization due to the electrical property differences between healthy and cancerous tissues[7]. For example, breast tumors often have higher conductivity than surrounding normal tissue, which originally motivated large clinical studies (>1000) that unfortunately suffered from low sensitivity (~25%)[124]. More recent studies using conformal electrode arrays[28] and improved reconstruction methods accommodating irregular shapes[125] report substantially improved sensitivity (>80%)[126].

Cardiovascular monitoring

The monitoring of heart health with EIT systems has previously been explored[127,128], but until now has been limited by the challenge of extracting the cardiac EIT signal from thoracic recordings. Compared to the lungs, EIT signatures of cardiac activity are smaller in magnitude, and often contain overlapping frequency content (heart rate vs breathing rate)[129]. Despite this, signal processing approaches such as decomposition techniques[130,131] and pixel-based clustering[66,132] have enabled the extraction of relatively clean cardiac EIT waveforms that have demonstrated agreement with invasive and noninvasive reference techniques in controlled settings.

Gastrointestinal motility

Another emerging area of EIT research is the monitoring of gastrointestinal (GI) function, such as gastric emptying and intestinal motility. GI motility disorders (e.g., gastroparesis, functional dyspepsia, or ileus) are often difficult to assess non-invasively, and current tests can be cumbersome (scintigraphy, manometry) or indirect. By placing an EIT electrode belt around

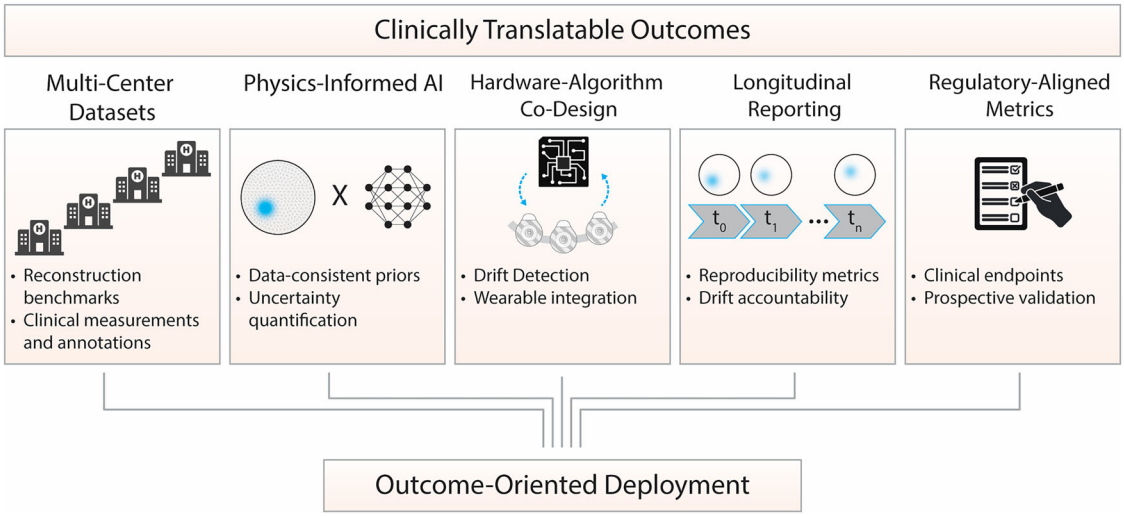


Fig. 6 | Roadmap for clinically translatable EIT deployment. Priorities for transitioning EIT from research-based reconstruction to outcome-oriented clinical deployment include shared multicenter datasets, integration of physics-informed AI, hardware-algorithm co-design for wearable integration, standardized longitudinal reporting frameworks, and regulatory-aligned performance metrics focused on clinical endpoints. Together, these efforts support outcome-oriented deployment across hospital, community, and home environments. Some images were created in BioRender. *Edelman, B.* (2026) https://BioRender.com/ajkeelo.

the abdomen, feasibility studies could track gastric emptying of liquids by observing the decline in stomach content over time[133]. Moreover, a wearable "gastric EIT" system was recently developed that can monitor meal-related changes in gastric volume and motility non-invasively in healthy subjects[134]. While feasibility has been demonstrated, standardized performance benchmarks and outcome-based validation studies are currently lacking.

Validation considerations

Together, Tier 3 applications function as stress tests for EIT's capabilities; however, across all maturity tiers, a central translational challenge lies in establishing clinical equivalence or additive value relative to established reference standards. For ventilation monitoring, outcome-based trials are emerging; however, for abdominal, neurological, and oncological applications, validation often relies on correlation with MRI, CT, elastography, or laboratory biomarkers, and there remains a need for predefined clinical endpoints[15,57,118,128]. Future progress will require standardized acquisition protocols and prospective studies that evaluate sensitivity, specificity, and longitudinal reproducibility across diverse populations.

Hardware-algorithm design for wearable and decentralized EIT

Wearable EIT architectures

Wearable deployment fundamentally alters the operating assumptions of EIT systems. Traditional EIT systems often rely on cart-based consoles with wired electrode belts, limiting use to hospital or research environments. Next-generation platforms integrate compact electronics, wireless data transmission, and mobile device connectivity[38]. Specifically, the integration of low-power electronics[9] and energy harvesting technology[135] into wearable EIT devices has been central to this evolution, allowing them to operate for extended periods without the need for frequent recharging. Moreover, innovative electrode designs, including "cooperative" or active electrodes, aim to minimize the noise footprint of sensors while maintaining ergonomics appropriate for a wearable device[58,136]. However, wearable deployment introduces additional engineering challenges that extend beyond simple miniaturization. Motion artifacts, variable belt positioning, and time-varying electrode-skin impedance can substantially degrade measurement consistency. Addressing these failure modes will require closed-loop signal quality monitoring that detect faulty electrodes due to suboptimal contact impedance and which accommodate varying levels of data quality through adaptive processing and reconstruction. In this context, wearable EIT development represents a scenario where hardware and algorithms must be designed together rather than sequentially optimized under clinical assumptions.

Decentralized monitoring and data infrastructure

The key translational question is not whether EIT can be made wearable, but whether impedance-derived biosignals remain stable across time, context, and individual[137]. Continuous impedance-based biosignals could provide early warning of deteriorating respiratory, cardiac, or metabolic function between scheduled clinical visits. Such a scheme is especially beneficial for patients with chronic metabolic or cardiopulmonary diseases, such as heart failure[138]. For such deployment to be viable, edge processing may be necessary to reduce data bandwidth and enable real-time artifact rejection prior to cloud transmission. Such a framework would thereby play a crucial role in remote diagnosis by providing imaging data to clinicians at frequent and regular intervals.

The long-term vision for decentralized EIT extends beyond passive monitoring. Integration with digital health platforms may enable continuous assessment of organ function in relation to lifestyle and environmental factors, allowing regular screenings to track physiological changes over time. Such monitoring could provide patients and clinicians with regular health updates and offer potential opportunities to guide lifestyle modifications aimed at stabilizing organ function or overall health. With this said, achieving this goal will require standardized reporting frameworks to ensure that longitudinal changes reflect physiology rather than acquisition variability. In addition, implementing robust cybersecurity measures and complying with data protection regulations will also be critical for maintaining patient trust and safeguarding sensitive health information.

Conclusion

Translational barriers

The evolution of EIT from an ICU monitoring tool toward decentralized functional imaging exposes five interdependent translational barriers. First, EIT remains constrained by a fundamental resolution-depth trade-off arising from the ill-posed inverse problem and exponential decay of sensitivity toward the imaging center. Hardware improvements and advanced regularization can mitigate, but not eliminate, this structural limitation. Second, boundary variability and the instability of the electrode-tissue interface introduce systematic uncertainty that becomes amplified in wearable and non-expert deployment contexts. Robust contact monitoring

and faulty electrode detection algorithms are therefore essential for reliable longitudinal use. Third, while AI-driven reconstruction and analysis have significantly improved visual fidelity and classification performance, shifts across devices and anatomies largely limit generalizability. Physics-informed or constraint-aware learning frameworks will likely be required to ensure measurement consistency. Fourth, longitudinal consistency within an individual and across populations have yet to be confirmed, and standardized acquisition protocols and multicenter benchmarking will be necessary to address gaps in this context. Finally, clinical translation across maturity tiers depends not only on technical feasibility but on rigorous prospective validation against established reference standards.

A roadmap for the next phase of EIT

Progress over the coming years will likely depend on coordinated advances across hardware, algorithms, and validation infrastructure (Fig. 6). Key priorities include:

- Development of shared multicenter datasets containing complementary clinical reference measurements and expert ground-truth annotations that enable objective benchmarking of reconstruction and biomarker performance.
- Integration of physics-informed AI models that enforce data consistency and provide calibrated uncertainty estimates.
- The co-design of hardware and algorithms for wearable systems with closed-loop signal quality monitoring and drift detection.
- Standardized reporting frameworks for longitudinal reproducibility.
- Regulatory-aligned performance metrics that emphasize clinical endpoints rather than only correlations.

If these challenges are addressed, EIT may transition from a niche bedside modality to a scalable platform for continuous functional surveillance across hospital, community, and home environments. Rather than competing with high-resolution structural imaging, the unique value of EIT will likely lie in safe, repeated, and dynamic physiological assessment that is both accessible and adaptable to different contexts and populations.

Data availability

No datasets were generated or analysed during the current study.

Received: 16 April 2026; Accepted: 12 September 2026;
Published online: 26 September 2026

References

1. Sakdinawat, A. & Attwood, D. Nanoscale X-ray imaging. *Nat. Photon.* **4**, 840–848 (2010).
2. Wald, L. L., McDaniel, P. C., Witzel, T., Stockmann, J. P. & Cooley, C. Z. Low-cost and portable MRI. *J. Magn. Reson. Imaging* **52**, 686–696 (2020).
3. Hoskins, P., Martin, K. & Thrush, A. *Diagnostic Ultrasound, Third Edition: Physics and Equipment*. (CRC Press, 2019).
4. Du, Y. et al. NeuroMark: an automated and adaptive ICA based pipeline to identify reproducible fMRI markers of brain disorders. *Neuroimage Clin.* **28**, 102375 (2020).
5. Edelman, B. J. & Macé, E. Functional ultrasound brain imaging: bridging networks, neurons, and behavior. *Curr. Opin. Biomed. Eng.* **18**, 100286 (2021).
6. Gallezot, J.-D., Lu, Y., Naganawa, M. & Carson, R. E. Parametric Imaging With PET and SPECT. *IEEE Trans. Radiat. Plasma Med. Sci.* **4**, 1–23 (2020).
7. Brown, B. H. Electrical impedance tomography (EIT): a review. *J. Med. Eng. Technol.* **27**, 97–108 (2003).
8. Li, J. H. W. et al. An all-inclusive electrical impedance tomography system for remote disease monitoring of multiple vital organs. Preprint at *medRxiv* https://doi.org/10.64898/2026.04.27.26351830 (2026).
9. Yang, L. et al. A wireless, low-power, and miniaturized EIT system for remote and long-term monitoring of lung ventilation in the isolation ward of ICU. *IEEE Trans. Instrum. Meas.* **70**, 1–11 (2021).
10. Khan, T. A. & Ling, S. H. Review on electrical impedance tomography: artificial intelligence methods and its applications. *Algorithms* **12**, 88 (2019).
11. Cebrian Carcavilla, A. & Meribout, M. Algorithms on electrical impedance tomography, focusing on deep learning architectures and their implementations: a review. *IEEE Sens. J.* **25**, 34252–34274 (2025).
12. Huang, J.-J., Hung, Y.-H., Wang, J.-J. & Lin, B.-S. Design of wearable and wireless electrical impedance tomography system. *Measurement* **78**, 9–17 (2016).
13. Kim, K. et al. Extremely durable electrical impedance tomography–based soft and ultrathin wearable e-skin for three-dimensional tactile interfaces. *Sci. Adv.* **10**, eadr1099 (2024).
14. Lasarow, L. et al. Regional lung function measures determined by electrical impedance tomography during repetitive ventilation manoeuvres in patients with COPD. *Physiol. Meas.* **42**, 015008 (2021).
15. Li, J. H. W. et al. Machine learning enabled portable electrical impedance tomography system for community-level chronic kidney disease classification and eGFR estimation. In *Proc. 47th Annual International Conference of the IEEE Engineering in Medicine and Biology Society* (IEEE, 2025).
16. Chang, C.-C. et al. Electrical impedance tomography for non-invasive identification of fatty liver infiltrate in overweight individuals. *Sci. Rep.* **11**, 19859 (2021).
17. Vonk-Noordegraaf, A. et al. Determination of stroke volume by means of electrical impedance tomography. *Physiol. Meas.* **21**, 285–293 (2000).
18. Brown, B. H. & Seagar, A. D. The Sheffield data collection system. *Clin. Phys. Physiol. Meas.* **8**, 91 (1987).
19. Brown, B. H. & Barber, D. C. Electrical impedance tomography; the construction and application to physiological measurement of electrical impedance images. *Med. Prog. Technol.* **13**, 69–75 (1987).
20. Ruan, W., Guardo, R. & Adler, A. Experimental evaluation of two iterative reconstruction methods for induced current electrical impedance tomography. *IEEE Trans. Med. Imaging* **15**, 180–187 (1996).
21. Tang, M., Wang, W., Wheeler, J., McCormick, M. & Dong, X. The number of electrodes and basis functions in EIT image reconstruction. *Physiol. Meas.* **23**, 129 (2002).
22. Schullcke, B., Krueger-Ziolek, S., Gong, B. & Moeller, K. Effect of the number of electrodes on the reconstructed lung shape in electrical impedance tomography. *Curr. Dir. Biomed. Eng.* **2**, 499–502 (2016).
23. Adler, A. & Boyle, A. Electrical impedance tomography: tissue properties to image measures. *IEEE Trans. Biomed. Eng.* **64**, 2494–2504 (2017).
24. Brazey, B., Haddab, Y. & Zemiti, N. Robust imaging using electrical impedance tomography: review of current tools. *Proc. R. Soc. A.* https://doi.org/10.1098/rspa.2021.0713 (2022).
25. Karsten, J., Stueber, T., Voigt, N., Teschner, E. & Heinze, H. Influence of different electrode belt positions on electrical impedance tomography imaging of regional ventilation: a prospective observational study. *Crit. Care* **20**, 3 (2016).
26. Shi, Y. et al. A mismatch correction method for electrode offset in electrical impedance tomography. *IEEE Sens. J.* **22**, 7248–7257 (2022).
27. Boyle, A. & Adler, A. The impact of electrode area, contact impedance and boundary shape on EIT images. *Physiol. Meas.* **32**, 745 (2011).
28. Um, S., Lee, J. & Yoo, H.-J. A 3.8-mW 1.9-mΩ/√Hz electrical impedance tomography ic with high input impedance and loading

effect calibration for 3-D early breast cancer detect system. *IEEE J. Solid-State Circuits* **59**, 2019–2028 (2024).
29. Land, K. J., Boeras, D. I., Chen, X.-S., Ramsay, A. R. & Peeling, R. W. REASSURED diagnostics to inform disease control strategies, strengthen health systems and improve patient outcomes. *Nat. Microbiol.* **4**, 46–54 (2019).
30. Home - Timpel precision ventilation. https://timpelmedical.com/en/ (2025).
31. Trastoy-Quintela, J. et al. Electric impedance tomography to monitor body positioning and chest physiotherapy in mechanically ventilated pediatric intensive care unit patients. *Sci. Rep.* **15**, 36741 (2025).
32. Dräger. Dräger PulmoVista® 500. https://www.draeger.com/de_ch/Products/PulmoVista-500.
33. sentecdev. Electrical impedance tomography (EIT) Device - LuMonTM. *Sentec* https://www.sentec.com/electrical-impedance-tomography/
34. Maltron. Electrical impedance tomography. Sheffield MK 3.5. https://maltronint.com/electrical-impedance-tomography/
35. Gense. AI portable health screening device. https://www.gensetechnologies.com
36. Kwok, W. C. et al. Lung function assessment by electrical impedance tomography among obese patients. *Sci. Rep.* **15**, 45337 (2025).
37. Chung, C. R. et al. Comparison of noninvasive cardiac output and stroke volume measurements using electrical impedance tomography with invasive methods in a swine model. *Sci. Rep.* **14**, 2962 (2024).
38. Hong, S. et al. A 4.9 mΩ-sensitivity mobile electrical impedance tomography IC for early breast-cancer detection system. *IEEE J. Solid-State Circuits* **50**, 245–257 (2015).
39. Zhu, Z. An overview of carbon nanotubes and graphene for biosensing applications. *Nano-Micro Lett.* **9**, 25 (2017).
40. Philipose, U. et al. Impedance analysis and noise measurements on multi walled carbon nanotube networks. *Materials* **14**, 7509 (2021).
41. Kuzum, D. et al. Transparent and flexible low noise graphene electrodes for simultaneous electrophysiology and neuroimaging. *Nat. Commun.* **5**, 5259 (2014).
42. Rabbani, K. S. & Kabir, A. M. B. H. Studies on the effect of the third dimension on a two-dimensional electrical impedance tomography system. *Clin. Phys. Physiol. Meas.* **12**, 393 (1991).
43. Wagenaar, J. & Adler, A. Electrical impedance tomography in 3D using two electrode planes: characterization and evaluation. *Physiol. Meas.* **37**, 922 (2016).
44. Kolehmainen, V., Vauhkonen, M., Karjalainen, P. A. & Kaipio, J. P. Assessment of errors in static electrical impedance tomography with adjacent and trigonometric current patterns. *Physiol. Meas.* **18**, 289 (1997).
45. Murai, T. & Kagawa, Y. Electrical impedance computed tomography based on a finite element model. *IEEE Trans. Biomed. Eng.* **32**, 177–184 (1985).
46. Babaeizadeh, S., Brooks, D. H., Isaacson, D. & Newell, J. C. Electrode boundary conditions and experimental validation for BEM-based EIT forward and inverse solutions. *IEEE Trans. Med. Imaging* **25**, 1180–1188 (2006).
47. Santosa, F. & Vogelius, M. A backprojection algorithm for electrical impedance imaging. *SIAM J. Appl. Math.* **50**, 216–243 (1990).
48. Gong, B., Schullcke, B., Krueger-Ziolek, S., Mueller-Lisse, U. & Moeller, K. Sparse regularization for EIT reconstruction incorporating structural information derived from medical imaging. *Physiol. Meas.* **37**, 843 (2016).
49. Mamatjan, Y., Borsic, A., Gürsoy, D. & Adler, A. An experimental clinical evaluation of EIT imaging with ℓ1 data and image norms. *Physiol. Meas.* **34**, 1027 (2013).
50. Vauhkonen, M., Vadasz, D., Karjalainen, P. A., Somersalo, E. & Kaipio, J. P. Tikhonov regularization and prior information in electrical impedance tomography. *IEEE Trans. Med. Imaging* **17**, 285–293 (1998).
51. Islam, Md. R. & Kiber, Md. A. Electrical impedance tomography imaging using Gauss–Newton algorithm. In *2014 International Conference on Informatics, Electronics & Vision* (*ICIEV*) 1–4 https://doi.org/10.1109/ICIEV.2014.6850719 (IEEE, 2014).
52. Wang, M. Inverse solutions for electrical impedance tomography based on conjugate gradients methods. *Meas. Sci. Technol.* **13**, 101 (2001).
53. Yang, D. et al. A DSP-based EIT system with adaptive boundary voltage acquisition. *IEEE Sens. J.* **22**, 5743–5754 (2022).
54. Jehl, M. & Holder, D. Correction of electrode modelling errors in multi-frequency EIT imaging. *Physiol. Meas.* **37**, 893 (2016).
55. Yang, L. et al. Removing clinical motion artifacts during ventilation monitoring with electrical impedance tomography: introduction of methodology and validation with simulation and patient data. *Front. Med.* **9**, 817590 (2022).
56. Zouari, F. et al. Global and regional lung function assessment using portable electrical impedance tomography (EIT) system: clinical study. In *2023 45th Annual International Conference of the IEEE Engineering in Medicine & Biology Society* (*EMBC*) 1–4 https://doi.org/10.1109/EMBC40787.2023.10340136 (IEEE, 2023).
57. Li, J. H. W. et al. Machine learning-assisted portable electrical impedance tomography enables accurate lung function assessment. *Annu. Int. Conf. IEEE Eng. Med. Biol. Soc.* **2025**, 1–4 (2025).
58. Wu, Y. et al. A high frame rate wearable EIT system using active electrode ASICs for lung respiration and heart rate monitoring. *IEEE Trans. Circuits Syst. Regul. Pap.* **65**, 3810–3820 (2018).
59. Nguyen, D. T., Jin, C., Thiagalingam, A. & McEwan, A. L. A review on electrical impedance tomography for pulmonary perfusion imaging. *Physiol. Meas.* **33**, 695 (2012).
60. Frerichs, I. & Becher, T. Chest electrical impedance tomography measures in neonatology and paediatrics—a survey on clinical usefulness. *Physiol. Meas.* **40**, 054001 (2019).
61. Zhao, Z., Pulletz, S., Frerichs, I., Müller-Lisse, U. & Möller, K. The EIT-based global inhomogeneity index is highly correlated with regional lung opening in patients with acute respiratory distress syndrome. *BMC Res. Notes* **7**, 82 (2014).
62. Spadaro, S. et al. Variation of poorly ventilated lung units (silent spaces) measured by electrical impedance tomography to dynamically assess recruitment. *Crit. Care* **22**, 26 (2018).
63. Hinz, J. et al. End-expiratory lung impedance change enables bedside monitoring of end-expiratory lung volume change. *Intensive Care Med.* **29**, 37–43 (2003).
64. Zouari, F. et al. Affordable, portable and self-administrable electrical impedance tomography enables global and regional lung function assessment. *Sci. Rep.* **12**, 20613 (2022).
65. Deibele, J. M., Luepschen, H. & Leonhardt, S. Dynamic separation of pulmonary and cardiac changes in electrical impedance tomography. *Physiol. Meas.* **29**, S1–S14 (2008).
66. Arshad, S. H. et al. Cardiac eigen imaging: a novel method to isolate cardiac activity in thoracic electrical impedance tomography. *Physiol. Meas.* **41**, 095008 (2020).
67. Adler, A. & Lionheart, W. R. B. Uses and abuses of EIDORS: an extensible software base for EIT. *Physiol. Meas.* **27**, S25 (2006).
68. Liu, B. et al. pyEIT: a python based framework for electrical impedance tomography. *SoftwareX* **7**, 304–308 (2018).
69. Hamilton, S. J. & Hauptmann, A. Deep D-bar: real time electrical impedance tomography imaging with deep neural networks. *IEEE Trans. Med. Imaging* **37**, 2367–2377 (2018).

70. Tan, C., Lv, S., Dong, F. & Takei, M. Image reconstruction based on convolutional neural network for electrical resistance tomography. *IEEE Sens. J.* **19**, 196–204 (2019).
71. Li, X. et al. One-dimensional convolutional neural network (1D-CNN) image reconstruction for electrical impedance tomography. *Rev. Sci. Instrum.* **91**, 124704 (2020).
72. Wang, Z. et al. Electrical impedance tomography image reconstruction with attention-based deep convolutional neural network. *IEEE Trans. Instrum. Meas.* **72**, 1–18 (2023).
73. Fu, R. et al. A regularization-guided deep imaging method for electrical impedance tomography. *IEEE Sens. J.* **22**, 8760–8771 (2022).
74. Gao, Y. et al. EIT-CDAE: a 2-D electrical impedance tomography image reconstruction method based on auto encoder technique. In *2019 IEEE Biomedical Circuits and Systems Conference* (*BioCAS*) 1–4 https://doi.org/10.1109/BIOCAS.2019.8918979 (IEEE, 2019).
75. Chen, R., Wu, W., Qi, H., Wang, J. & Wang, H. A stacked autoencoder neural network algorithm for breast cancer diagnosis with magnetic detection electrical impedance tomography. *IEEE Access* **8**, 5428–5437 (2020).
76. Zhang, K. et al. A deep generative model-integrated framework for 3-D time-difference electrical impedance tomography. *IEEE Trans. Instrum. Meas.* **72**, 1–12 (2023).
77. Li, X. et al. SAR-CGAN: improved generative adversarial network for EIT reconstruction of lung diseases. *Biomed. Signal Process. Control* **81**, 104421 (2023).
78. Ivanenko, M. et al. Image reconstruction using supervised learning in wearable electrical impedance tomography of the thorax. *Sensors* **23**, 7774 (2023).
79. Raza, O. et al. CycleGAN with mutual information loss constraint generates structurally aligned CT images from functional EIT images. In *2023 45th Annual International Conference of the IEEE Engineering in Medicine & Biology Society* (*EMBC*) 1–4 https://doi.org/10.1109/EMBC40787.2023.10340711 (IEEE, 2023).
80. Wang, Z. et al. Cross modality generative learning framework for anatomical transitive magnetic resonance imaging (MRI) from electrical impedance tomography (EIT) image. *Comput. Med. Imaging Graph.* **108**, 102272 (2023).
81. Liu, J., Shi, F., Xiong, H. & Zhou, Y. DiffusionEIT: diffusion model for electrical impedance tomography. *IEEE Trans. Instrum. Meas.* **73**, 1–9 (2024).
82. Shi, S., Kang, R. & Liatsis, P. A conditional diffusion model for electrical impedance tomography image reconstruction. *IEEE Trans. Instrum. Meas.* **74**, 1–16 (2025).
83. Tong, B., Wang, J. & Liu, D. Diff-INR: generative regularization for electrical impedance tomography. Preprint at https://doi.org/10.48550/arXiv.2409.04494 (2024).
84. Li, C. et al. DUMD-EIT: a three-stage deconvolution-UNet-masked diffusion model for electrical impedance tomography image reconstruction. In *Advanced Intelligent Computing Technology and Applications* (eds Huang, D.-S., Zhang, C., Zhang, Q. & Pan, Y.) 38–49 https://doi.org/10.1007/978-981-96-9869-1_4 (Springer Nature, 2025).
85. Liu, D., Wu, Y., Tong, B. & Deng, J. SDEIT: semantic-driven electrical impedance tomography. Preprint at https://doi.org/10.48550/arXiv.2504.04185 (2025).
86. Rädsch, T. et al. Labelling instructions matter in biomedical image analysis. *Nat. Mach. Intell.* **5**, 273–283 (2023).
87. Sylolypavan, A., Sleeman, D., Wu, H. & Sim, M. The impact of inconsistent human annotations on AI driven clinical decision making. *Npj Digit. Med.* **6**, 26 (2023).
88. Liu, D. et al. DeepEIT: deep image prior enabled electrical impedance tomography. *IEEE Trans. Pattern Anal. Mach. Intell.* **45**, 9627–9638 (2023).
89. Fang, H. et al. D2IP: deep dynamic image prior for 3D time-sequence pulmonary impedance imaging. Preprint at https://doi.org/10.48550/arXiv.2507.14046 (2025).
90. Vahabi, N. et al. Deep analysis of EIT dataset to classify apnea and non-apnea cases in neonatal patients. *IEEE Access* **9**, 25131–25139 (2021).
91. Chen, S. et al. Spatio-temporal classification of lung ventilation patterns using 3D EIT images: a general approach for individualized lung function evaluation. *IEEE J. Biomed. Health Inform.* **28**, 367–378 (2024).
92. Cansiz, B., Kilinc, C. U. & Serbes, G. Deep learning-driven feature engineering for lung disease classification through electrical impedance tomography imaging. *Biomed. Signal Process. Control* **100**, 107124 (2025).
93. Ye, J. et al. Removal of vibration interference artifacts in electrical impedance tomography monitoring using residual learning strategy. *IEEE Trans. Instrum. Meas.* **73**, 1–10 (2024).
94. Ren, S., Guan, R., Liang, G. & Dong, F. RCRC: a deep neural network for dynamic image reconstruction of electrical impedance tomography. *IEEE Trans. Instrum. Meas.* **70**, 1–11 (2021).
95. Song, Z. et al. Pulmonary electrical impedance tomography based on deep recurrent neural networks. Preprint at https://doi.org/10.48550/arXiv.2504.14521 (2025).
96. Strodthoff, N., Strodthoff, C., Becher, T., Weiler, N. & Frerichs, I. Inferring respiratory and circulatory parameters from electrical impedance tomography with deep recurrent models. *IEEE J. Biomed. Health Inform.* **25**, 3105–3111 (2021).
97. Cappellini, I., Campagnola, L. & Consales, G. Electrical impedance tomography, artificial intelligence, and variable ventilation: transforming respiratory monitoring and treatment in critical care. *J. Pers. Med.* **14**, 677 (2024).
98. Zhu, L., Lu, W., Soleimani, M., Li, Z. & Zhang, M. Electrical impedance tomography guided by digital twins and deep learning for lung monitoring. *IEEE Trans. Instrum. Meas.* **72**, 1–9 (2023).
99. Wisse, J. J. et al. Clinical implementation of advanced respiratory monitoring with esophageal pressure and electrical impedance tomography: results from an international survey and focus group discussion. *Intensive Care Med. Exp.* **12**, 93 (2024).
100. Becher, T. et al. Individualization of PEEP and tidal volume in ARDS patients with electrical impedance tomography: a pilot feasibility study. *Ann. Intensive Care* **11**, 89 (2021).
101. Franchineau, G. et al. Bedside contribution of electrical impedance tomography to setting positive end-expiratory pressure for extracorporeal membrane oxygenation–treated patients with severe acute respiratory distress syndrome. *Am. J. Respir. Crit. Care Med.* **196**, 447–457 (2017).
102. Jimenez, J. V. et al. Electric impedance tomography-guided PEEP titration reduces mechanical power in ARDS: a randomized crossover pilot trial. *Crit. Care* **27**, 21 (2023).
103. He, H. et al. Early individualized positive end-expiratory pressure guided by electrical impedance tomography in acute respiratory distress syndrome: a randomized controlled clinical trial. *Crit. Care* **25**, 230 (2021).
104. Chatziioannidis, I., Samaras, T. & Nikolaidis, N. Electrical impedance tomography: a new study method for neonatal respiratory distress syndrome? *Hippokratia* **15**, 211–215 (2011).
105. Frerichs, I., Schiffmann, H., Hahn, G. & Hellige, G. Non-invasive radiation-free monitoring of regional lung ventilation in critically ill infants. *Intensive Care Med.* **27**, 1385–1394 (2001).
106. Pillow, J. J., Frerichs, I. & Stocks, J. Lung function tests in neonates and infants with chronic lung disease: global and regional ventilation inhomogeneity. *Pediatr. Pulmonol.* **41**, 105–121 (2006).
107. Gaertner, V. D., Mühlbacher, T., Waldmann, A. D., Bassler, D. & Rüegger, C. M. Early prediction of pulmonary outcomes in preterm

infants using electrical impedance tomography. *Front. Pediatr.* **11**, 1167077 (2023).
108. Davies, P., Yasin, S., Gates, S., Bird, D. & Silvestre, C. Clinical scenarios of the application of electrical impedance tomography in paediatric intensive care. *Sci. Rep.* **9**, 5362 (2019).
109. Soltész, L. et al. EIT guided evaluation of regional ventilation distributions in neonatal and pediatric ARDS: a prospective feasibility study. *Respir. Res.* **26**, 60 (2025).
110. Schaefer, M. S. et al. Electrical impedance tomography during major open upper abdominal surgery: a pilot-study. *BMC Anesthesiol.* **14**, 51 (2014).
111. Buonanno, P. et al. Electric impedance tomography and protective mechanical ventilation in elective robotic-assisted laparoscopy surgery with steep Trendelenburg position: a randomized controlled study. *Sci. Rep.* **13**, 2753 (2023).
112. Chen, L. et al. Electrical impedance tomography-guided positive end-expiratory pressure titration for perioperative oxygenation and postoperative pulmonary complications: a systematic review and meta-analysis. *Medicine* **103**, e40357 (2024).
113. Li, Z. et al. Evaluation of mechanical ventilation modes in the laparoscopic perioperative period with electrical impedance tomography. *PLoS ONE* **20**, e0331194 (2025).
114. Yang, L., Lin, Q., Zhao, Z. & Zhang, J. Early detection of pulmonary aspiration during anesthetic induction via bedside electrical impedance tomography monitoring: a case report. *JCA Adv.* **2**, 100137 (2025).
115. Yap, D. Y. H. et al. Bio-conductivity characteristics of chronic kidney disease stages examined by portable frequency-difference electrical impedance tomography. In *2022 44th Annual International Conference of the IEEE Engineering in Medicine & Biology Society* (*EMBC*) 3378–3381 https://doi.org/10.1109/EMBC48229.2022.9871377 (IEEE, 2022).
116. Li, J. H. W. et al. Machine learning enabled portable electrical impedance tomography system for community level chronic kidney disease classification and eGFR estimation. *Annu. Int. Conf. IEEE Eng. Med. Biol. Soc.* **2025**, 1–4 (2025).
117. Luo, Y. et al. Non-invasive electrical impedance tomography for multi-scale detection of liver fat content. *Theranostics* **8**, 1636–1647 (2018).
118. Bahukhandi, R. et al. AI-enabled electrical impedance tomography (EIT) system for detecting and quantifying metabolic associated steatotic liver disease. *Annu. Int. Conf. IEEE Eng. Med. Biol. Soc.***2025**, 1–4 (2025).
119. Goren, N. et al. Multi-frequency electrical impedance tomography and neuroimaging data in stroke patients. *Sci. Data* **5**, 180112 (2018).
120. Dowrick, T., Blochet, C. & Holder, D. In vivo bioimpedance measurement of healthy and ischaemic rat brain: implications for stroke imaging using electrical impedance tomography. *Physiol. Meas.* **36**, 1273 (2015).
121. Dowrick, T., Blochet, C. & Holder, D. In vivo bioimpedance changes during haemorrhagic and ischaemic stroke in rats: towards 3D stroke imaging using electrical impedance tomography. *Physiol. Meas.* **37**, 765 (2016).
122. Hannan, S. et al. Imaging fast electrical activity in the brain during ictal epileptiform discharges with electrical impedance tomography. *Neuroimage Clin.* **20**, 674–684 (2018).
123. Hannan, S. et al. Imaging slow brain activity during neocortical and hippocampal epileptiform events with electrical impedance tomography. *Physiol. Meas.* **42**, 014001 (2021).
124. Stojadinovic, A. et al. Electrical impedance scanning as a new breast cancer risk stratification tool for young women. *J. Surg. Oncol.* **97**, 112–120 (2008).
125. He, J. et al. Three-dimensional image reconstruction of breast tumor by electrical impedance tomography based on dimensional Grey Wolf optimization algorithm. *IEEE Trans. Instrum. Meas.* **74**, 1–10 (2025).
126. Du, Z., Wan, H., Chen, Y., Pu, Y. & Wang, X. Bioimpedance spectroscopy can precisely discriminate human breast carcinoma from benign tumors. *Medicine* **96**, e5970 (2017).
127. Braun, F. et al. Limitations and challenges of EIT-based monitoring of stroke volume and pulmonary artery pressure. *Physiol. Meas.* **39**, 014003 (2018).
128. Lawson, M. et al. Portable electrical impedance tomography enables heart ejection fraction measurement for health screening in nonspecialist settings. *Proc. 47th Annu. Int. Conf. IEEE Eng. Med. Biol. Soc.* **2025**, 1–4 (2025).
129. Graf, M. & Riedel, T. Electrical impedance tomography: amplitudes of cardiac related impedance changes in the lung are highly position dependent. *PLoS ONE* **12**, e0188313 (2017).
130. Jang, G. Y. et al. Noninvasive, simultaneous, and continuous measurements of stroke volume and tidal volume using EIT: feasibility study of animal experiments. *Sci. Rep.* **10**, 11242 (2020).
131. Ko, R. E. et al. Noninvasive beat-to-beat stroke volume measurements to determine preload responsiveness during mini-fluid challenge in a swine model: a preliminary study. *Shock* **56**, 850–856 (2021).
132. Trepte, C. J. C. et al. Electrical impedance tomography for non-invasive assessment of stroke volume variation in health and experimental lung injury. *Br. J. Anaesth.* **118**, 68–76 (2017).
133. Nakae, Y. et al. Cold pain prolongs gastric emptying of liquid but not solid meal: an electrical impedance tomography (EIT) study. *J. Gastroenterol.* **35**, 593–597 (2000).
134. Sakai, K. et al. Gastric functional monitoring by gastric electrical impedance tomography (gEIT) suit with dual-step fuzzy clustering. *Sci. Rep.* **13**, 514 (2023).
135. Yang, P. et al. A wearable triboelectric impedance tomography system for noninvasive and dynamic imaging of biological tissues. *Sci. Adv.* **10**, eadr9139 (2024).
136. Rapin, M. et al. Wearable sensors for frequency-multiplexed EIT and multilead ECG data acquisition. *IEEE Trans. Biomed. Eng.* **66**, 810–820 (2019).
137. Noh, H. W., Sim, J. Y., Ahn, C.-G. & Ku, Y. Electrical impedance of upper limb enables robust wearable identity recognition against variation in finger placement and environmental factors. *Biosensors* **11**, 398 (2021).
138. Giménez-Miranda, L. et al. Wearable devices based on bioimpedance test in heart failure: clinical relevance: systematic review. *Rev. Cardiovasc. Med.* **25**, 315 (2024).

Acknowledgements

We thank Eddie C. Wong and Kannie W. Y. Chan for useful discussions and comments.

Author contributions

R.W.C. initiated and led the preparation of this manuscript. R.W.C. and B.J.E. defined the scope of the review and delineated the topics to be discussed in this work. M.L., H.L., B.J.E. and R.W.C. wrote the manuscript. M.L., H.L., C.M.H., D.Y.H.Y., W.K.S., B.J.E. and R.W.C. reviewed, edited, and approved the final manuscript.

Competing interests

R.W.C., B.J.E., and W.K.S. declare no competing non-financial interests, but declare the following competing financial Interests: R.W.C. is a co-founder and shareholder of E-SENSE Innovation & Technology Ltd., Hong Kong, China. B.J.E. is an employee/contractor and shareholder of E-SENSE Innovation & Technology Ltd., Hong Kong, China. W.K.S. received research funding via the University of Hong Kong from Pfizer, AstraZeneca, 89Bio, Ribo Life Sciences and Boehringer Ingelheim, received speaker's fees and research funding from Echosens and MSD, is an advisory board member

and received speaker's fees from Abbott and Gilead Sciences. M.L., H.L., C.M.H., and D.Y.H.Y. declare no competing financial or non-financial interests.

Additional information

Correspondence and requests for materials should be addressed to Bradley J. Edelman or Russell W. Chan.

Reprints and permissions information is available at http://www.nature.com/reprints

Publisher's note Springer Nature remains neutral with regard to jurisdictional claims in published maps and institutional affiliations.

Open Access This article is licensed under a Creative Commons Attribution-NonCommercial-NoDerivatives 4.0 International License, which permits any non-commercial use, sharing, distribution and reproduction in any medium or format, as long as you give appropriate credit to the original author(s) and the source, provide a link to the Creative Commons licence, and indicate if you modified the licensed material. You do not have permission under this licence to share adapted material derived from this article or parts of it. The images or other third party material in this article are included in the article's Creative Commons licence, unless indicated otherwise in a credit line to the material. If material is not included in the article's Creative Commons licence and your intended use is not permitted by statutory regulation or exceeds the permitted use, you will need to obtain permission directly from the copyright holder. To view a copy of this licence, visit http://creativecommons.org/licenses/by-nc-nd/4.0/.

© The Author(s) 2026

This Article in Press is shared early to give you faster access to new research. It is citable and carries a permanent DOI. The final edited version will replace it automatically.